Catalytic Mechanism of New TiC-Doped Sodium Alanate for Hydrogen Storage

Xuezhang Xiao, Xiulin Fan, Kairong Yu, Shouquan Li, Changpin Chen, Qidong Wang, and Lixin Chen*

Department of Materials Science and Engineering, Zhejiang University, Hangzhou 310027, PR China

Received: July 29, 2009; Revised Manuscript Received: October 15, 2009

TiC as a novel catalyst was used in preparing TiC-doped sodium aluminum hydride by ball-milling NaH/Al mixture or $NaAlH_4$ with TiC powder under a hydrogen atmosphere. It is found that TiC-doped NaH/Al composite absorbs 4.77 wt % hydrogen at 120 °C, desorbs more than 80% hydrogen of its initial hydrogen capacity at 155 °C with a stable cycling dehydriding rate and capacity, and exhibits better reversible hydrogen storage properties than those of TiC-doped $NaAlH_4$ composite or Ti-doped NaH/Al composite. The catalytic mechanism of TiC for reversible hydrogen storage behavior of TiC-doped sodium aluminum has been studied through XRD and SEM-EDS analyses. The experiment led us believe that the refined TiC particles inlaid on the surface of a larger hydride matrix act not only as the catalytic active sites for the redox reaction of hydrogen, and act as the hydrogen spillover for hydrogen diffusion, but also prevent the growth in size of small spherical alanate, resulting in the improvement of hydriding/dehydriding properties of the sodium alanate system.

1. Introduction

Sodium alanate has been regarded as one of the promising hydrogen storage materials since the first stimulating work by Bogdanović et al. in 1997 on the excellent hydrogen storage property of Ti-doped $NaAlH_4$ under moderate conditions of pressure and temperatures.[1] Ti-doped $NaAlH_4$ has been investigated intensively for hydrogen fuel-cell applications because of its high theoretical hydrogen weight capacity of 5.6 wt % and its high availability.[2,3] After being doped with a Ti-based compound, $NaAlH_4$ complex hydride can store and release hydrogen reversibly at 100−150 °C in two steps according to the following reactions,[1]

$$3NaH + 3Al + 4.5H_2 \leftrightarrow Na_3AlH_6 + 2Al + 3H_2 \leftrightarrow 3NaAlH_4 \quad (1)$$

At the present time, the available reversible hydrogen storage capacity (around 4.0 wt %) is less than the theoretical capacity (5.6 wt %) due to the poor hydriding/dehydriding kinetics of the $NaAlH_4$ system. After being doped with a suitable catalyst, such as $Ti(OBu^n)_4$, $TiCl_3$, or $ScCl_3$, the reaction kinetics of $NaAlH_4$ is improved obviously.[4−6] However, utilization of these precursors with high-valence Ti-compounds as dopants generally gives birth to some inactive reaction byproducts (e.g., sodium-oxide and sodium-chloride), which are dead weight products in the system, resulting in a significant reduction of practically available hydrogen storage weight percentage.[7] Therefore, the development of a new catalyst and an effective doping method to enhance the reaction kinetics of $NaAlH_4$ without generating dead weight byproducts becomes an important direction of research for the alanate system. Recently, Wang et al. developed a new method to dope $NaAlH_4$ by ball-milling NaH/Al mixture with metallic Ti powder.[8] This method of using Ti powder as the dopant has the advantage over that doped with high-valence Ti-compounds in the elimination of inactive byproducts. However, the hydrogen storage capacity reported by this Ti-doped $NaAlH_4$ sample was below 4.0 wt % H_2 due to the lower catalytic activity of coarse grained metallic Ti particle.[8,9] Besides metallic Ti, other possible Ti-compounds, such as TiN and TiO_2 in the form of nanopowder, have been tested as catalysts to provide an improved dehydriding property of $NaAlH_4$ without generating any byproducts for achieving a higher reversible storage capacity (about 5 wt %).[10,11] However, the reaction kinetics of TiN-doped $NaAlH_4$ is too slow to be considered as a viable candidate for fuel-cell applications, and the cycling hydrogen storage properties of TiO_2-doped $NaAlH_4$ are yet unclear.

Furthermore, although it has been reported that many catalysts can improve the hydrogen storage properties of $NaAlH_4$ effectively, the mechanisms for these catalytic enhancements are yet unclear.[4−6,10−16] There are mainly two different mechanisms reported for enhancement of the reaction kinetics of $NaAlH_4$ with dopants. One belongs to the Ti or Ti−Al active species acting as a classic catalyst for hydrogen dissociation/recombination on the surface of reacting solids.[4,12,13] The other belongs to the substitution of Ti from dopant for Na and/or Al element in the bulk hydride lattice to cause lattice distortions.[14−16] Until now, there are fewer investigations on the catalytic mechanism of the Ti-doped $NaAlH_4$ system than there are on their dehydriding properties. It is well-known that catalytic improvement of the hydriding or hydrogenation process (forward reaction 1) is very important for the development of complex hydrides as on-board hydrogen storage materials.

In addition, it was reported that graphite as a codopant of titanium-based catalyst enhanced significantly both the hydrogenation and the dehydrogenation kinetics of catalyzed $NaAlH_4$.[17] TiC is known for being very hard and brittle, and it is a very stable compound with a high Ti−C bond enthalpy of 423 kJ/mol.[18] Hence, we believe that the hard and brittle TiC particle, as a single dopant combined with high-energy ball-milling technology in the $NaAlH_4$ system, might enhance the ball-milling efficiency and increase the defects in the $NaAlH_4$

* To whom correspondence should be addressed. Tel./Fax: +86 571 8795 1152. E-mail: lxchen@zju.edu.cn (L.X.C.).

10.1021/jp907258p CCC: $40.75
Published on Web 11/04/2009

matrix. Moreover, the strong bonding strength of Ti−C would prevent TiC from reacting with $NaAlH_4$ to create any dead weight and hydrocarbon pollution in this system. With these advantages in mind, we decided to use TiC powder as the dopant to prepare TiC-doped $NaAlH_4$ (NaH/Al) composite with high-energy ball-milling, and then to investigate the hydriding/dehydriding properties and the catalytic mechanism of this system in the present article.

2. Experimental Section

The starting materials used in this study were $NaAlH_4$ powder (95%), NaH powder (95%, ~74 ~im), Al powder (99%, 74−154 ~im), and TiC powder (99%, <4 ~im), all purchased from Sigma-Aldrich Co. and used as received. To intensify the catalysis of TiC and visualize its catalytic mechanism, the amount of TiC doped into the $NaAlH_4$ or NaH/Al (NaH and Al with a mole ratio of 1:1) was made up to 10 mol % to assure that some TiC phases can be detected in X-ray diffraction analysis. The mixtures of TiC-doped $NaAlH_4$ ($NaAlH_4$ + 10 mol % TiC) and TiC-doped NaH/Al (NaH/Al + 10 mol % TiC) composites were carefully introduced into a stainless steel vessel together with stainless steel balls and milled in a planetary ball mill for 48 h. The vessel was evacuated first and then filled with supra-pure hydrogen at 0.6 MPa. The ball-to-powder weight ratio was 30:1. All sample loading and unloading were carried out in the glovebox under purified argon atmosphere.

Hydriding/dehydriding properties of the doped samples were tested on a Sievert's type apparatus. Each time before the hydriding test, the sample was heated up to 165 °C under vacuum in about 0.5 h to ensure a complete dehydrogenation. The hydriding test was carried out under the initial hydrogen pressure of 9−12 MPa at about 85−140 °C, and the dehydriding temperature was determined at 155 °C against 0.1 MPa. The reversible hydrogen storage capacity was calculated in weight percent on the basis of the changes in hydrogen volumes and pressures in the reactor and finally normalized to the weight of $NaAlH_4$ (NaH/Al) with the weight of TiC included.

The crystal structures and surface morphology were performed with X-ray diffraction (XRD, ARL X'TRA, Thermo Electron Corp.) and scanning electron microscopy (SEM, HITACHI S-4800) with an energy dispersive analysis for X-rays (EDS). The sample was covered with a special plastic tape to prevent its direct contact with water vapor and oxygen during measurement.

3. Results and Discussion

Figure 1 shows the hydriding/dehydriding curves of TiC-doped $NaAlH_4$ and TiC-doped NaH/Al composites in the first cycle. It is interesting to find that a pronounced improvement in the hydriding/dehydriding properties of the $NaAlH_4$ (NaH/Al) samples can be achieved by being ball-milled with TiC. As presented in Figure 1, the TiC-doped NaH/Al and dehydrided TiC-doped $NaAlH_4$ composites can absorb 4.77 and 4.41 wt % hydrogen in 10 h at 120 °C with 11.5 MPa hydriding pressure, respectively. However, the NaH/Al composite ball-milled under the same condition without TiC hardly absorbs hydrogen. A similar observation is found for the composites dehydrided at 155 °C; the hydrided TiC-doped NaH/Al composite and the TiC-doped $NaAlH_4$ composite release 3.85 and 3.11 wt % hydrogen, respectively. It should be pointed out that the pure $NaAlH_4$ had released about 0.2 wt % hydrogen in 10 h at 155 °C during its initial dehydrogenation. Thus it indicates that TiC powder as a dopant plays a critical role in the improvement of hydriding/dehydriding properties in the $NaAlH_4$ (NaH/Al) system Moreover, it is interesting to note from the curves in Figure 1 that the slopes of the hydriding/dehydriding curves of TiC-doped NaH/Al composite are steeper than those of TiC-doped $NaAlH_4$, suggesting that TiC-doped NaH/Al composite exhibits higher hydriding/dehydriding rates. The phenomenon that doping a catalytic agent into the dehydrided product (NaH/Al here) improves the hydriding/dehydriding kinetics more effectively, compared to the direct doping into the hydrided product ($NaAlH_4$ here), is in agreement with the results of Wang et al.[9] We believe that doping TiC powder into NaH/Al instead of $NaAlH_4$ would produce a more homogeneous dispersion of active particles on the surface of the alanate matrix.[19] On the grounds of this observation, we utilized this advanced way of introducing catalyst into a NaH and Al mixture in the subsequent investigations.

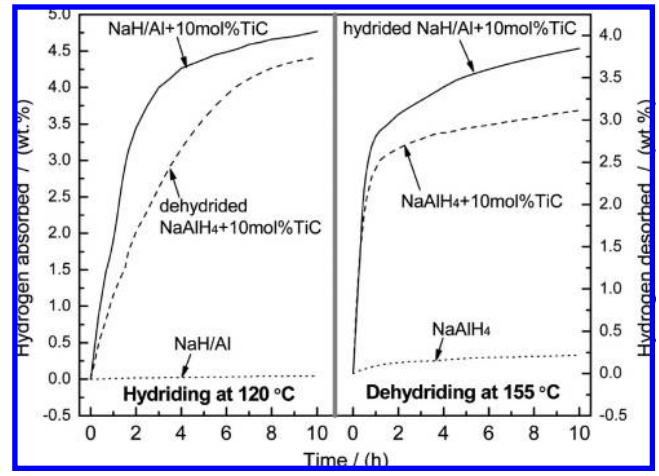

Figure 1. Hydriding/dehydriding curves of TiC-doped $NaAlH_4$ and TiC-doped NaH/Al composites in the first cycle.

Recently, it has been reported that metallic Ti could catalytically improve the hydrogen storage property of $NaAlH_4$.[19,20] For comparison purposes, the metallic Ti powder was also chosen as a dopant to prepare a Ti-doped NaH/Al composite, and its hydriding properties were compared with those of the TiC-doped NaH/Al composite. The cycling hydrogen storage properties between TiC-doped NaH/Al and Ti-doped NaH/Al composites under different hydrogenation conditions are presented in Table 1. The hydriding capacity listed in Table 1 is defined as the amount of hydrogen absorbed under the initial hydriding temperature and pressure in a specified time. The TiC-doped NaH/Al composite reaches a higher hydriding capacity of 4.06−4.76 wt % during the initial temperature of 118−130 °C and pressure of 10−12 MPa (in the 1st through 5th cycles). As the initial hydriding temperature and pressure decrease to 85−100 °C and 9−9.6 MPa respectively, the hydriding capacity reduces to 2.83−3.07 wt %, as the hydriding kinetics of the composite becomes worse under the lower hydriding temperature and pressure. For the Ti-doped NaH/Al composite, its hydriding capacities ranged from 2.27 to 4.23 wt % under a temperature of 100−140 °C and pressure of 7.5−13.5 MPa (in the 1st through 9th cycles), and its hydriding capacity increases with the increase of hydriding temperature from 85 to 120 °C (in the 8th through 10th cycles). Therefore, it can be concluded from Table 1 that the catalytic activity of TiC is higher than that of Ti for the improvement of hydrogen storage properties of sodium alanate hydride, as both the hydriding rate and capacity of TiC-doped NaH/Al composite are higher than those of the Ti-doped NaH/Al composite. For example, the TiC-doped NaH/Al composite absorbs 4.12 wt % hydrogen in 6 h, whereas

TABLE 1: Comparison of Cycling Hydriding Properties between TiC-Doped NaH/Al and Ti-Doped NaH/Al Composites

	NaH/Al + 10 mol % TiC			NaH/Al + 10 mol % Ti[c]		
cycle no.	hydrogenation conditions (°C[a]/MPa[b])	hydriding time (h)	hydriding capacity (wt %)	hydrogenation conditions (°C[a]/MPa[b])	hydriding time (h)	hydriding capacity (wt %)
1	120/11.5	8	4.62	120/13.5	7.5	3.49
2	120/11.5	5.5	4.08	120/13	7.5	3.62
3	125/11	6	4.12	125/11	6	3.19
4	118/10	5	4.06	120/13.5	9	4.23
5	130/12	8	4.76	140/13.5	6.5	3.76
6	140/11.8	3.5	3.96	120/9	7	2.98
7	120/11	4.5	3.86	120/7.5	4.8	2.27
8	120/10	4	3.83	120/13.5	5	3.41
9	100/9	6.5	3.07	100/10.8	6	3.02
10	85/9.6	10	2.83	85/13.5	7	2.58

[a] Initial hydriding temperature. [b] Initial hydriding pressure. [c] Data obtained from refs 20−22.

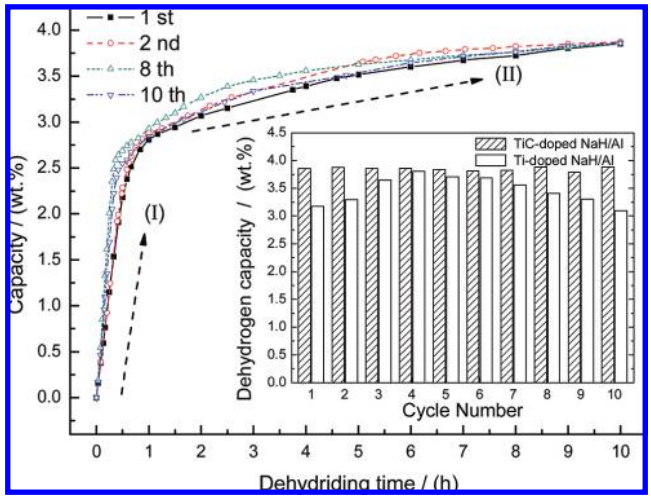

Figure 2. Cycling dehydriding curves of hydrided TiC-doped NaH/Al composite tested at 155 °C against 0.1 MPa for 8 h (comparison of the dehydriding capacities between TiC-doped NaH/Al and Ti-doped NaH/Al composites in the first 10 cycles are presented in the insert).

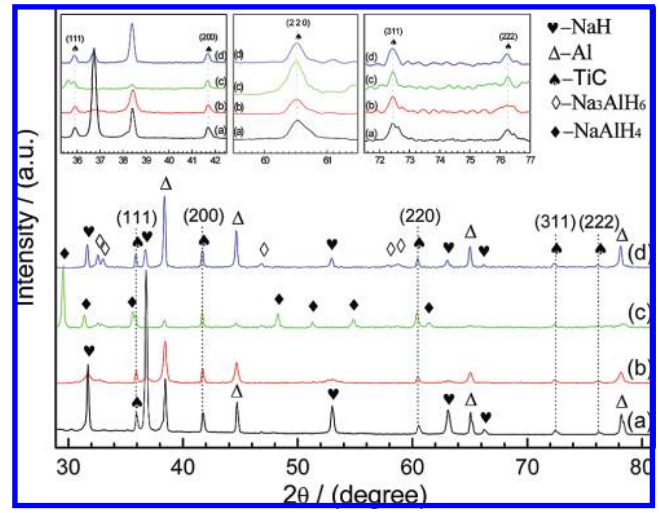

Figure 3. XRD patterns of the TiC-doped NaH/Al composite in different ball-milling and cycling hydriding/dehydriding stages. (a) Before ball-milling, (b) after ball-milling, (c) after hydrogenation of the first cycle, and (d) after dehydrogenation of the first cycle.

the Ti-doped NaH/Al composite absorbs only 3.19 wt % under the same hydrogenation conditions at the third cycle. Also, the TiC-doped NaH/Al composite absorbs 3.83 wt % even under the lower hydriding pressure of 10 MPa with a shorter hydriding time of 4 h, whereas the Ti-doped NaH/Al composite absorbs only 3.41 wt % hydrogen under a hydriding pressure and time of 13.5 MPa and 5 h respectively at the 8th cycle.

The cycling dehydriding curves of hydrided TiC-doped NaH/Al composite are shown in Figure 2. The dehydrogenation process was carried out at 155 °C against 0.1 MPa after the composite was hydrided at 120 °C and 13.5 MPa H_2 in 10 h. It is found that the dehydriding rate is slightly improved after the first cycle, with no sign of obvious degradation of dehydriding kinetics of TiC-doped NaH/Al composite in the first 10 cycles. The dehydriding curves clearly show that there are two different chemical reaction steps in the reverse reaction 1, as marked out by the dashed lines with arrow heads in Figure 2. All dehydriding curves are composed of two parts: a faster reaction part (I) corresponding to the dehydrogenation of $NaAlH_4$, and a slower reaction part (II) corresponding to the dehydrogenation of Na_3AlH_6.[22] Moreover, it can be seen that the cycling dehydriding capacities of hydrided TiC-doped NaH/Al composite are all higher than that of hydrided Ti-doped NaH/Al composite with the same dehydriding time of 10 h, as shown in the insert of Figure 2. We ascribe the higher dehydriding capacity together with the stable reaction rate of the hydrided TiC-doped NaH/Al composite possibly to the presence of a large number of defects and larger specific surface areas in the $NaAlH_4$ system caused by the doped brittle TiC particle during ball-milling. The stable and brittle TiC particles can act as the catalytic species in the whole dehydrogenation process, because these TiC particles do not react with $NaAlH_4$ hydride matrix to generate any invalid byproduct. That will be discussed in XRD analysis later. Although the TiC-doped NaH/Al composite has stable cycling hydriding/dehydriding capacities, its initial hydriding and dehydriding capacities in current study, around 4.77 and 3.85 wt %, as shown in Figure 1, are still below the theoretical hydrogen capacity of ~5.0 wt % (taking into account the TiC powder weight in the composite during calculation) in the TiC-doped $NaAlH_4$ system. Further research efforts, aimed in particular toward improving the reversible cycling hydrogen capacity and hydriding/dehydriding rate through using nanosized TiC as catalyst, changing TiC doping content, codoping with multiple-catalysts, and modifying the $NaAlH_4$ system structure will be presented in forthcoming publications.

Figure 3 shows the XRD patterns of TiC-doped NaH/Al composite in different ball-milling and cycling hydriding/dehydriding stages. Before ball-milling, the NaH and Al main phases with strong diffraction peaks as well as the minor phase of TiC in the (NaH/Al + TiC) mixture are all shown in part a of Figure 3. After ball-milling, TiC-doped NaH/Al composite consists of NaH and Al together with TiC phases, but the diffraction intensities of NaH and Al peaks become greatly

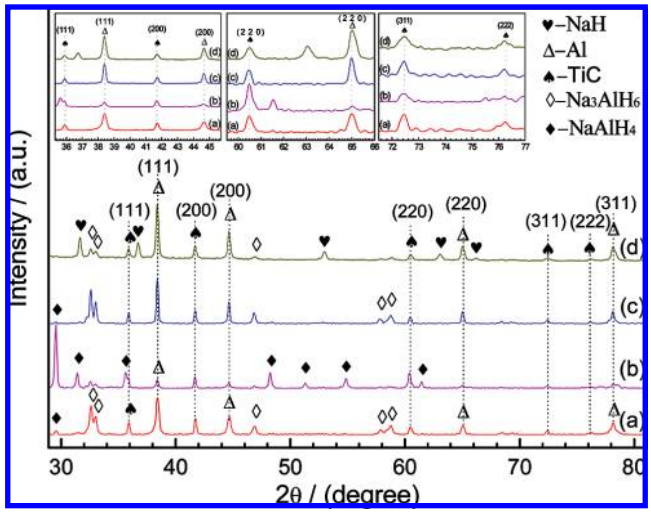

Figure 4. XRD patterns of the TiC-doped NaH/Al composite in different cycling hydriding/dehydriding stages. (a) Intermediate hydrogenation (hydrided for 1 h) of the 10th cycle, (b) after hydrogenation of the 10th cycle, (c) intermediate dehydrogenation (dehydrided for 1 h) of the 10th cycle, and (d) after dehydrogenation of the 10th cycle.

weakened and broadened, whereas the diffraction intensity of TiC peaks remain unchanged, as shown in part b of Figure 3. This indicates that the grain size of the NaH/Al matrix decreases greatly and a large number of defects are formed in the ball-milled composite. It is remarkable to note that the diffraction intensity of NaH in ball-milled composite decreases dramatically and becomes lower than that of Al, suggesting that the grain size of the NaH powder is decreased sharply, as the brittle NaH hydride particle is more easily crushed than the ductile Al metal during ball milled with TiC powder, and the ductile Al particles incline to be clad onto several smaller NaH particles to form the integral composite. After being hydrogenated, the main phases change from NaH and Al to $NaAlH_4$. The main phases change back to NaH and Al again after dehydrogenation. There are a few Na_3AlH_6 diffraction peaks both in the hydrogenated/dehydrogenated samples (as shown in parts c and d of Figure 3). It confirms that the hydriding/dehydriding process of TiC-doped NaH/Al composite is reversible, but the hydrogenation/dehydrogenation reactions are not complete. This phenomenon is similar to that occurring in the $TiCl_3$-doped $NaAlH_4$ system.[23] The XRD patterns of the TiC-doped NaH/Al composite in different hydriding/dehydriding stages of the 10th cycle are also shown in Figure 4. At the 10th cycle, $NaAlH_4$ still exists as the main phase in the sample after hydrogenation (as shown in part b of Figure 4), and NaH and Al are changing to the main phases after complete dehydrogenation (as shown in part d of Figure 4). This result further suggests that the TiC-doped $NaAlH_4$ system possesses good reversibility, and according to reaction 1 even the hydrogenation/dehydrogenation cycling extends to 10 cycles. Moreover, the Na_3AlH_6 interphase can be found in the intermediate hydrogenation/dehydrogenation processes (as shown in parts a and c of Figure 4). This confirms that reversible hydriding/dehydriding reactions are a two-step process according to reaction 1 as mentioned above.

The mechanism for the catalysis of the Ti compound improving the hydrogen storage property of $NaAlH_4$ has been extensively investigated. It has been reported that the classic Ti-halides (such as $TiCl_3$) are able to react with $NaAlH_4$ or NaH/Al to form $TiAl_x$ (such as $TiAl_3$), which acts as the catalyst responsible for hydrogen dissociation/recombination at the surface of hydride with the migration of the Al diffraction peak moving toward the high-angle side after the ball-milling and hydriding/dehydriding processes.[4,13,24,25] It is interesting to note that the (111), (200), (220), (311), and (222) diffraction peaks of TiC and the (111), (200), (220), and (311) diffraction peaks of Al all remain after the hydrogenation and dehydrogenation processes. It means that TiC and Al maintain their original phase structures in different hydriding/dehydriding stages throughout (namely, before hydrogenation, intermediate hydrogenation/dehydrogenation, and after complete hydrogenation/dehydrogenation), as shown from the three magnified XRD patterns in the inserts of Figure 3 and Figure 4. These results proved that TiC had not reacted with $NaAlH_4$ or NaH/Al in this study, and no $TiAl_x$ alloy was formed during the ball-milling and hydriding/dehydriding processes. Therefore, it can be inferred that the catalytic mechanism of doping with TiC as catalyst into the $NaAlH_4$ system to improve its hydriding/dehydriding properties is different from that of doping with classic $TiCl_3$ as catalyst. Combining the results of the above-mentioned hydrided/dehydrided properties of TiC-doped NaH/Al ($NaAlH_4$) composite and the results of our previous investigation,[20,22] we believe that TiC fine particles are existing stably and separatively around the hydride matrix as the catalytically active species for reversible the hydrogen storage process of the composite. Because TiC powder is thermodynamically more stable than other Ti-chloride catalysts,[26,27] utilization of this stable TiC catalyst can be identified as an effective way to catalytically enhance the cycling hydriding/dehydriding properties of TiC-doped NaH/Al composite without generating any dead weight byproduct, for which the catalystic mechanism is similar to that of TiN[10] and TiO_2[11].

Up to now, both the experimental and theoretical investigations on the hydrogenation of NaH/Al (forward reaction 1) for reversible hydrogen storage process are rather limited[24,25,28,29] compared with those on the dehydrogenation of $NaAlH_4$ (reverse reaction 1). To clearly reveal the catalytic mechanism of TiC for the improvement of hydriding/dehydriding properties in TiC-doped NaH/Al composite, we finally resorted to the microstructure analysis of the Ti powder, the TiC powder, and the TiC-doped NaH/Al composite in different hydrogenation stages by using SEM. It can be seen from SEM images of Ti and TiC in parts a and b of Figure 5 that the particle sizes of TiC powder (ranging from 0.2 to 3 μm) are smaller than that of Ti powder (ranging from 1 to 50 μm). It is reasonable to believe that, as a dopant precursor, the finer TiC would distribute among the hydride matrix more homogeneously than Ti, and then facilitates the dissociation/recombination of hydrogen in TiC-doped NaH/Al composite.[11] Prior to ball-milling, the irregular flaky NaH particles (ranging from 10 to 40 μm) and granular Al particles (ranging from 15 to 35 μm) can be seen distinctly in the composite, whereas the TiC particles cannot be seen clearly because of their smaller dimensions and lower content. After ball-milling, the angular features of individual NaH and Al particles are completely gone, and the shape of the composite changes into small spherical particles of about $1-10$ μm in size. This indicates that the brittle NaH hydride particles are reduced to a small particle and clad with the ductile Al. Because of the interaction between the continuously deformated metallic powder and the fractured brittle powder during ball-milling,[27] we believe that the much larger specific surface area, resulting from the greatly reduced particle size in the ball-milled composite, would increase the hydriding/dehydriding reaction activity sites and hence would be beneficial to the enhancement of hydrogen storage kinetics as shown in Figure 1. However,

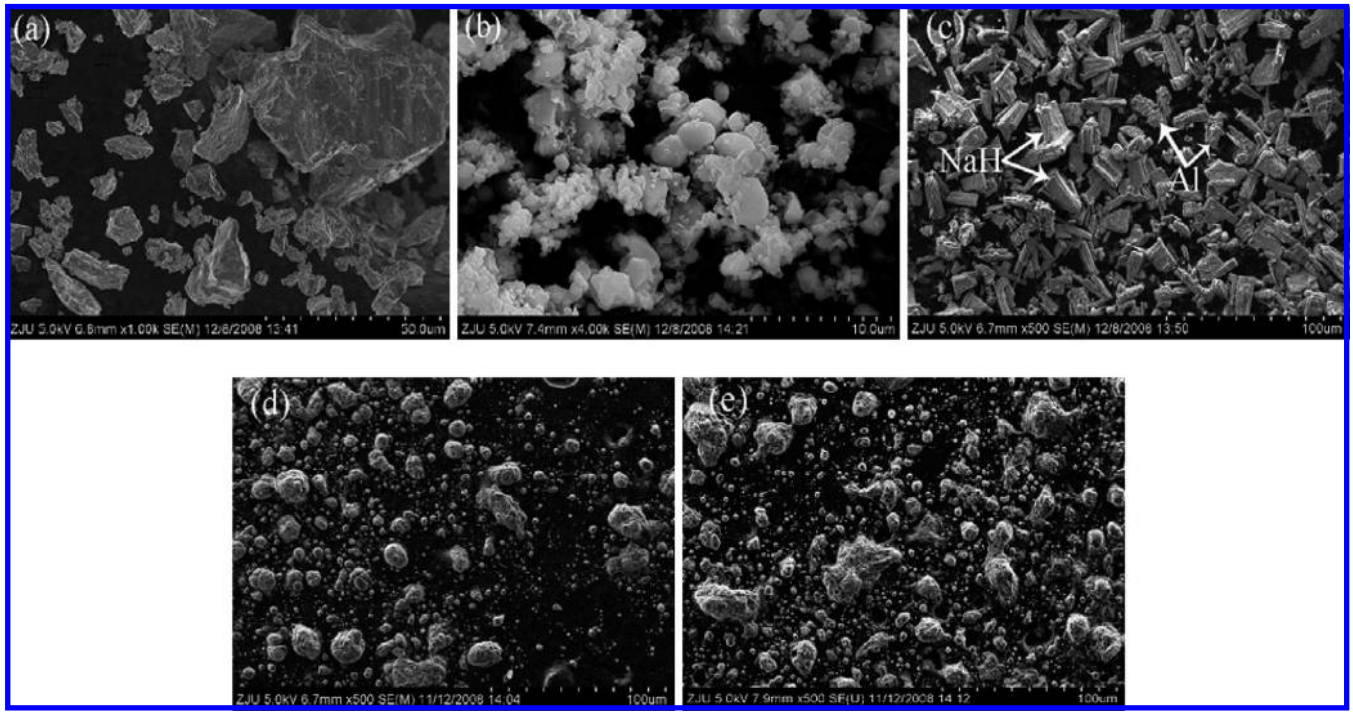

Figure 5. SEM images of Ti powder, TiC powder, and TiC-doped NaH/Al composite in different ball-milling and hydrogenation stages; (a) Ti powder, (b) TiC powder, (c) TiC-doped NaH/Al composite before ball-milling, (d) TiC-doped NaH/Al after ball-milling (before hydrogenation), and (e) TiC-doped NaH/Al composite after hydrogenation of the 10th cycle.

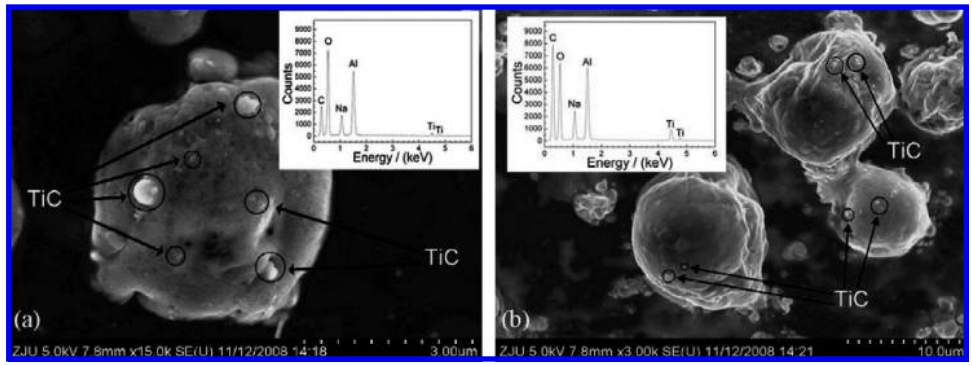

Figure 6. SEM-EDS results of the TiC-doped NaH/Al composite before and after hydrogenation. (a) Before hydrogenation (after ball-milling) and (b) after hydrogenation of the 10th cycle.

in part c of Figure 5 there are a few larger particles in size over 20 μm, which presumably are formed by the agglomeration of Al and NaH powder resulting from a longer ball-milling process.[30] In addition, although the agglomerations reunited from small particles are still present in the dehydrided composite after 10 cycles as seen in part e of Figure 5, it can also be found that the average particle size of the composite remains unchanged and most particles maintain in fine size.

Figure 6 shows the magnified SEM images and surface EDS results of TiC-doped NaH/Al composite before and after hydrogenation. It can be seen from part a of Figure 6 that there are several bright small particles (ranging from 50 to 400 nm) inlaid on the surface of the larger hydride globelet matrix after ball-milling, and there are several distinct wrinkles on the surface, which increase effectively the contact area between the composite and hydrogen. According to the representative EDS analysis of the bright particles dispersed on the matrix surface shown in the insert of Figure 6 together with the magnified XRD patterns in part b of Figure 3 and part b of Figure 4, the bright spots should be identified as small TiC particles. Recent research on hydrogen exchange kinetics based on John-Mehl-Avrami (JMA) analysis indicates that the rate-limiting step for hydrogenation/dehydrogenation reaction of the $NaAlH_4$ system doped with Ti-compound catalyst is determined by a diffusion-controlled growth process.[31] In this study, the refined TiC catalyst particles inlaid in the matrix facilitate hydrogen diffusion into the (NaH/Al) composite and provide also interfaces for the nucleation and diffusion of Na_3AlH_6 and $NaAlH_4$.[23] Moreover, it can found from part b of Figure 6 that the distribution configuration of TiC catalyst particles on the matrix and the surface morphology and particle size of the $NaAlH_4$ matrix change very little after 10 hydrogenation/dehydrogenation cycles. This phenomenon contrasts markedly with the classical intermetallic compounds (e.g., $LaNi_5$ and TiFe), in which breakup and fragmentation are the important parts of the initial activation process in the first several cycles.[32,33] Thus it suggests that the stable hydriding/dehydriding properties of TiC-doped NaH/Al composite are associated with the fact that the matrix and catalyst of the composite could maintain their microstructure and particle configuration after many hydriding/dehydriding cycles.

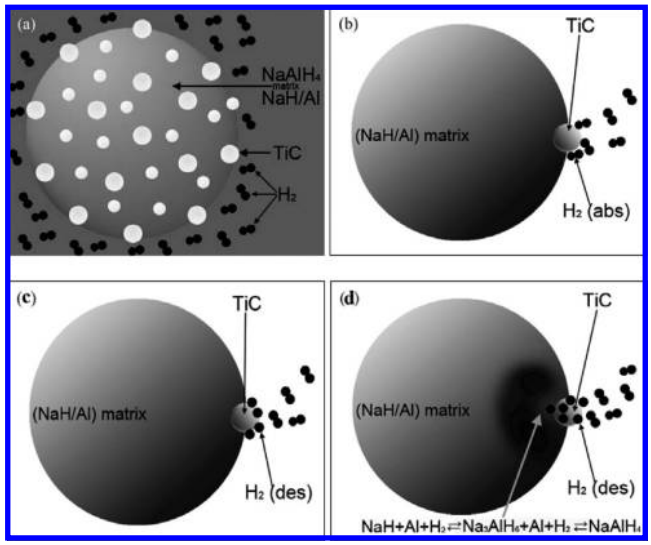

Figure 7. Scheme of TiC-doped NaH/Al composite in different states of hydrogenation. (a) Ball-milled NaH/Al ($NaAlH_4$) hydride matrix (big spheres) with inlaid TiC particles (small spheres), (b) adsorbed state of hydrogenation, (c) dissociated state of hydrogenation, and (d) diffused state of hydrogenation.

In conjunction with the above hydriding/dehydriding properties and microstructure analysis, we come to the conclusion that: (1) Ball-milled NaH/Al mixture with a few percent TiC catalysts can produce a favorable reactive composite consisting of NaH/Al in small globelets with sufficient area for contacting hydrogen and a large amount of defects acting as the reaction active sites. (2) The micronano TiC catalysts inlaid densely and homogeneously on the surface of the $NaAlH_4$(NaH/Al) matrix act as catalytic active species for hydriding/dehydriding reactions without producing any $TiAl_x$ alloy, which is different from the reported catalytic mechanism of transition-metal halides (e.g., $TiCl_3$ and TiF_3).[24,25] The scheme of TiC-doped NaH/Al composite in different states of hydrogenation is shown in Figure 7. From the above analysis, we believe that the smaller TiC particles inlaid on the surface of the larger NaH/Al matrix act not only as the catalytic active sites for the redox reaction of hydrogen but also as the hydrogen spillover for hydrogen diffusion into the matrix. As described in Figure parts b and d of 7, the catalytic hydrogenation process could be divided into three states: (i) hydrogen adsorption, the hydrogen molecules are preferentially adsorbed by the TiC catalysts inlaid on the surface of NaH/Al matrix (as shown in part b of Figure 7); (ii) hydrogen dissociation, the hydrogen molecules are subsequently dissociated into hydrogen atoms around the TiC active sites (as shown in part c of Figure 7); (iii) hydrogen diffusion, most hydrogen atoms preferentially diffuse into the NaH/Al matrix through the hydrogen spillover provided by the TiC active species (as shown in part d of Figure 7). From the XRD and SEM-EDS analyses, it is found that the ratio of constituent for NaH and Al is inhomogeneous after ball-milling as a portion of NaH particles are clad by Al in the matrix. We believe that the TiC-doped NaH/Al composite hydrogen would be adsorbed more easily by the inlaid TiC catalysts and then diffuse into the NaH and Al through the interface of TiC and the NaH/Al matrix to form Na_3AlH_6 and $NaAlH_4$ complex hydrides. Similarly, the catalytic dehydrogenation process in this system is carried out following the reverse order of the above three hydrogenation reaction steps. (3) In addition, it has been reported that the $NaAlH_4$ hydride particles would grow into the larger ones as the hydrogenation/dehydrogenation cycling number increases, which results in the gradual deterioration of reversible hydrogen storage properties.[35] In the case of TiC-doped NaH/Al composite, we believe also that the hard and brittle TiC particles dispersed stably on the entire surface of hydrides matrix would suppress the agglomeration of small particles into larger ones and thus preserve the stable reaction kinetic properties in the subsequent hydriding/dehydriding cycles.

4. Conclusions

The hydriding/dehydriding properties and microstructures of Ti-doped $NaAlH_4$(NaH/Al) complex hydrides prepared by ball-milling $NaAlH_4$ or NaH/Al with TiC powder were investigated systematically. The TiC powder as a dopant plays a critical role in the improvement of hydriding/dehydriding properties of the sodium alanate system. The TiC-doped NaH/Al composite exhibits a noticeable improvement of cycling hydrogen storage properties. Its initial hydriding/dehydriding capacities increase 4.77 wt % (at 120 °C) and 3.85 wt % (at 155 °C) respectively, together with a more stable hydriding/dehydriding rate and capacity on cycling. XRD and SEM-EDS analyses show that micronano TiC particles inlaid on the surface of a larger spherical NaH/Al matrix act not only as the catalytic active sites for the redox reaction of hydrogen but also as the hydrogen spillover for hydrogen diffusion into the matrix. It is interesting to note that in the catalytic hydrogenation process three reaction states are occurring simultaneously: (i) hydrogen molecules are adsorbed by the TiC catalysts inlaid on the surface of the NaH/Al matrix, (ii) hydrogen molecules are dissociated into hydrogen atoms around the TiC active sites, and (iii) hydrogen atoms preferentially diffuse into the NaH/Al matrix through the hydrogen spillover provided by the TiC active species. The catalytic dehydrogenation process is carried out following the reverse order and path of the above hydrogenation reaction. In addition, the hard and brittle TiC particles dispersed stably on the surface of the hydride matrix effectively suppress the particles' agglomeration, and thus a high reaction kinetics is preserved during cycling.

Acknowledgment. We acknowledge financial support from the National Basic Research Program of China (Grant No. 2007CB209701), from the China Postdoctoral Science Foundation (Grant No. 20080440196, 200902622), from the National Natural Science Foundation of China (Grant Nos. 50871099, 50631020), and the Program for New Century Excellent Talents in Universities (Grant No. NCET-07-0741).

References and Notes

(1) Bogdanović, B.; Schwickardi, M. *J. Alloys Compd.* **1997**, *253*, 1.
(2) Bogdanović, B.; Eberle, U.; Schwickardi, M.; Schüth, F. *Scr. Mater.* **2007**, *56*, 813.
(3) Jensen, J. O.; Li, Q.; Pan, C.; Vestbo, A. P.; Mortensen, K.; Nybo, P. H.; Lau, S. C.; Nedergaard, C. T.; Schramm, J.; Bjerrum, N. J. *Int. J. Hydrogen Energy* **2007**, *32*, 1567.
(4) Bogdanović, B.; Brand, R. A.; Marjanovic, A.; Schwickardi, M.; Tolle, J. *J. Alloys Compd.* **2000**, *302*, 36.
(5) Majzoub, E. H.; Gross, K. J. *J. Alloys Compd.* **200**, *356*, 363.
(6) Bogdanović, B.; Felderhoff, M.; Pommerin, A.; Schüth, T.; Spielkamp, N. *Adv. Mater.* **2006**, *18*, 1198.
(7) Suttisawat, Y.; Jannatisin, V.; Rangsunvigit, P.; Kitiyanan, B.; Muangsin, N.; Kulprathipanja, S. *J. Power Sources* **2007**, *163*, 997.
(8) Wang, P.; Jensen, C. M. *J. Phys. Chem. B* **2004**, *108*, 15827.
(9) Wang, P.; Kang, X. D.; Cheng, H. M. *J. Phys. Chem. B* **2005**, *109*, 20131.
(10) Bogdanović, B.; Felderhoff, M.; Kaskel, S.; Pommerin, A.; Schlichte, K.; Schüth, F. *Adv. Mater.* **2003**, *15*, 1012.
(11) Lee, G. J.; Shim, J. H.; Cho, Y. W.; Lee, K. S. *Int. J. Hydrogen Energy* **2008**, *33*, 3748.
(12) Majzoub, E. H.; McCarty, K. F.; Ozolins, V. *Phys. Rev. B* **2005**, *71*, 024118.

(13) Fang, F.; Zhang, J.; Zhu, J.; Chen, G. R.; Sun, D. L.; He, B.; Wei, Z.; Wei, S. Q. *J. Phys. Chem. C* **2007**, *111*, 3476.
(14) Sun, D. L.; Kiyobayashi, T.; Takeshita, H. T.; Kuriyama, N.; Jensen, C. M. *J. Alloys Compd.* **2002**, *337*, L8.
(15) Lovvik, O. M.; Opalka, S. A. *Phys. Rev. B* **2005**, *71*, 054103.
(16) Araujo, C. M.; Ahuja, R.; Guillen, J. M. O.; Jena, P. *Appl. Phys. Lett.* **2005**, *86*, 251913.
(17) Wang, J.; Ebner, A. D.; Prozorov, T.; Zidan, R.; Ritter, J. A. *J. Alloys Compd.* **2005**, *395*, 252.
(18) Tong, J.; Magtoto, N.; Kelber, J. *Appl. Surf. Sci.* **2003**, *220*, 203.
(19) Wang, P.; Kang, X. D.; Cheng, H. M. *J. Phys. Chem. B* **2005**, *109*, 20131.
(20) Xiao, X. Z.; Chen, L. X.; Wang, X. H.; Wang, Q. D.; Chen, C. P. *Int. J. Hydrogen Energy* **2007**, *32*, 2475.
(21) Xiao, X. Z.; Chen, L. X.; Wang, X. H.; Li, S. Q.; Chen, C. P. *Acta Phys-Chim. Sin.* **2006**, *22*, 1511.
(22) Xiao, X. Z.; Chen, L. X.; Wang, X. H.; Li, S. Q.; Wang, Q. D.; Chen, C. P. *Int. J. Hydrogen Energy* **2007**, *32*, 3954.
(23) Brinks, H. W.; Sulic, M.; Jensen, C. M.; Hauback, B. C. *J. Phys. Chem. B* **2006**, *110*, 2740.
(24) Bogdanović, B.; Felderhoff, M.; Germann, M.; Hartel, M.; Pommerin, A.; Schüth, F.; Weidenthaler, C.; Zibrowius, B. *J. Alloys Compd.* **2003**, *350*, 246.
(25) Brinks, H. W.; Hauback, B. C.; Srinivasan, S. S.; Jensen, C. M. *J. Phys. Chem. B* **2005**, *109*, 15780.
(26) Gross, K. J.; Sandrock, G.; Thomas, G. J. *J. Alloys Compd.* **2002**, *330*, 691.
(27) Eigen, N.; Kunowsky, M.; Klassen, T.; Bormann, R. *J. Alloys Compd.* **2008**, *465*, 310.
(28) Fang, F.; Zheng, S. Y.; Chen, G. R.; Sang, G.; He, B.; Wei, S. Q.; Sun, D. L. *Acta Mater.* **2009**, *57*, 1959.
(29) Chaudhuri, S.; Graetz, J.; Ignatov, A.; Reilly, J. J.; Muckerman, J. T. *J. Am. Chem. Soc.* **2006**, *128*, 11404.
(30) Thomas, G. J.; Gross, K. J.; Yang, N. Y. C.; Jensen, C. M. *J. Alloys Compd.* **2002**, *330*, 702.
(31) Kircher, O.; Fichtner, M. *J. Appl. Phys.* **2004**, *95*, 7748.
(32) Wang, X. H.; Wang, C. Y.; Chen, C. P.; Wang, Q. D. *J. Alloys Compd.* **2006**, *420*, 107.
(33) Ma, J. X.; Pan, H. G.; Wang, X. H.; Chen, C. P.; Wang, Q. D. *Int. J. Hydrogen Energy* **2000**, *25*, 779.
(34) Kang, X. D.; Wang, P.; Cheng, H. M. *Int. J. Hydrogen Energy* **2007**, *32*, 2943.
(35) Sakintuna, B.; Lamari-Darkrim, F.; Hirscher, M. *Int. J. Hydrogen Energy* **2007**, *32*, 1121.

JP907258P